Received 11 February; accepted 18 March 2002; doi:10.1038/nature00803.

1. Baglioni, C. Chromosomal and cytoplasmic regulation of haemoglobin synthesis. *Bibl. Haemat.* **29,** 1056–1063 (1966).
2. Nathan, D. G. & Gunn, R. B. Thalassemia: the consequences of unbalanced hemoglobin synthesis. *Am. J. Med.* **41,** 815–830 (1966).
3. Rachmilewitz, E. & Schrier, S. L. in *Disorders of Haemoglobin* (eda Steinberg, M. H., Forget, B. G., Higgs, D. R. & Nagel, R. L.) 233–251 (Cambridge Univ. Press, Cambridge, 2001).
4. Weiss, M. J. & Orkin, S. H. GATA transcription factors: Key regulators of hematopoiesis. *Exp. Hematol.* **23,** 99–107 (1995).
5. Shirihai, O. S., Gregory, T., Yu, C., Orkin, S. H. & Weiss, M. J. ABC-me, a novel mitochondrial transporter induced by GATA-1 during erythroid differentiation. *EMBO J.* **19,** 2492–2502 (2000).
6. Weiss, M. J., Keller, G. & Orkin, S. H. Novel insights into erythroid development revealed through in vitro differentiation of GATA-1^{-} embryonic stem cells. *Genes Dev.* **8,** 1184–1197 (1994).
7. Fujiwara, Y., Browne, C. P., Cunniff, K., Goff, S. C. & Orkin, S. H. Arrested development of embryonic red cell precursors in mouse embryos lacking transcription factor GATA-1. *Proc. Natl Acad. Sci. USA* **93,** 12355–12358 (1996).
8. Miele, G., Manson, J. & Clinton, M. A novel erythroid-specific marker of transmissible spongiform encephalopathies. *Nature Med.* **7,** 361–364 (2001).
9. Nathan, D. G., Stossel, T. B., Gunn, R. B., Zarkowsky, H. S. & Laforet, M. T. Influence of hemoglobin precipitation on erythrocyte metabolism in alpha and beta thalassemia. *J. Clin. Invest.* **48,** 33–41 (1969).
10. Shinar, E., Shalev, O., Rachmilewitz, E. A. & Schrier, S. L. Erythrocyte membrane skeleton abnormalities in severe beta-thalassemia. *Blood* **70,** 158–164 (1987).
11. Sorensen, S., Rubin, E., Polster, H., Mohandas, N. & Schrier, S. The role of membrane skeletal-associated alpha-globin in the pathophysiology of beta-thalassemia. *Blood* **75,** 1333–1336 (1990).
12. Yuan, J. *et al.* The instability of the membrane skeleton in thalassemic red blood cells. *Blood* **86,** 3945–3950 (1995).
13. Yuan, J. *et al.* Accelerated programmed cell death (apoptosis) in erythroid precursors of patients with severe beta-thalassemia (Cooley's anemia). *Blood* **82,** 374–377 (1993).
14. Pootrakul, P. *et al.* A correlation of erythrokinetics, ineffective erythropoiesis, and erythroid precursor apoptosis in Thai patients with thalassemia. *Blood* **96,** 2606–2612 (2000).
15. Centis, F. *et al.* The importance of erythroid expansion in determining the extent of apoptosis in erythroid precursors in patients with beta-thalassemia major. *Blood* **96,** 3624–3629 (2000).
16. Rachmilewitz, E. A., Peisach, J. & Blumberg, W. E. Studies on the stability of oxyhemoglobin A and its constituent chains and their derivatives. *J. Biol. Chem.* **246,** 3356–3366 (1971).
17. Wickramasinghe, S. N. & Hughes, M. Ultrastructural studies of erythropoiesis in beta-thalassaemia trait. *Br. J. Haematol.* **46,** 401–407 (1980).
18. Ciavatta, D. J., Ryan, T. M., Farmer, S. C. & Townes, T. M. Mouse model of human beta zero thalassemia: targeted deletion of the mouse beta maj- and beta min-globin genes in embryonic stem cells. *Proc. Natl Acad. Sci. USA* **92,** 9259–9263 (1995).
19. Yang, B. *et al.* A mouse model for beta (0)-thalassemia. *Proc. Natl Acad. Sci. USA* **92,** 11608–11612 (1995).
20. Shaeffer, J. R. Evidence for soluble alpha-chains as intermediates in hemoglobin synthesis in the rabbit reticulocyte. *Biochem. Biophys. Res. Commun.* **28,** 647–652 (1967).
21. Tavill, A. S., Grayzel, A. I., Vanderhoff, G. A. & London, I. M. The control of hemoglobin synthesis. *Trans. Assoc. Am. Physic.* **80,** 305–313 (1967).
22. Prusiner, S. B., Scott, M. R., DeArmond, S. J. & Cohen, F. E. Prion protein biology. *Cell* **93,** 337–348 (1998).
23. Wickner, S., Maurizi, M. R. & Gottesman, S. Posttranslational quality control: folding, refolding, and degrading proteins. *Science* **286,** 1888–1893 (1999).
24. Bank, A. & O'Donnell, J. V. Intracellular loss of free α chains in β-thalassaemia. *Nature* **222,** 295–296 (1969).
25. Shaeffer, J. R. Turnover of excess hemoglobin α chains in β-thalassemic cells is ATP-dependent. *J. Biol. Chem.* **258,** 13172–13177 (1983).
26. Huang, S.-C. & Benz, E. J. in *Disorders of Haemoglobin* (eds Steinberg, M. H., Forget, B. G., Higgs, D. R. & Nagel, R. L.) 146–173 (Cambridge Univ. Press, Cambridge, 2001).
27. Gregory, T. *et al.* GATA-1 and erythropoietin cooperate to promote erythroid cell survival by regulating bcl-x_L expression. *Blood* **94,** 87–96 (1999).
28. Ikeda-Saito, M., Inubushi, T. & Yonetani, T. in *Hemoglobins* (eds Antonini, E., Rossi-Bernardi, L. & Chiancone, E.) 113–121 (Academic, New York, 1981).
29. Rachmilewitz, E. A. Denaturation of the normal and abnormal hemoglobin molecule. *Semin. Hematol.* **11,** 441–462 (1974).

Supplementary Information accompanies the paper on *Nature*'s website (http://www.nature.com/nature).

Acknowledgements

We thank S. Krishnaswamy for advice and assistance in biochemical studies and use of equipment, J. Yu and Z. He for technical assistance, D. Speicher for assistance with protein sequencing, C. Clendenin for assistance with mouse blastocyst injections, T. Labosky for providing embryonic stem cells, and D. Nathan, D. Pellman and W. Englander for helpful discussions and review of the manuscript. This work was funded by grants from the Cooley's Anemia Foundation (M.J.W.), the Unico Foundation (M.J.W.) and the National Institutes of Health (M.J.W., J.E.R. and G.A.B.) M.J.W. is a recipient of The American Society of Hematology Junior Faculty Award.

Competing interests statement

The authors declare that they have no competing financial interests

Correspondence and requests for materials should be addressed to M.J.W. (e-mail: weissmi@email.chop.edu).

Regulation of *Arabidopsis* cryptochrome 2 by blue-light-dependent phosphorylation

Dror Shalitin*, Hongyun Yang*, Todd C. Mockler*, Maskit Maymon*, Hongwei Guo†, Garry C. Whitelam‡ & Chentao Lin*

** Department of Molecular, Cell & Developmental Biology, University of California, Los Angeles, California 90095, USA*
‡ Biology Department, University of Leicester, Leicester LE1 7RH, UK
† Present address: Genomic Analysis Laboratory, The Salk Institute for Biological Studies, 10010 N. Torrey Pines Road, La Jolla, California 92037, USA.

Cryptochromes are blue/ultraviolet-A light receptors that mediate various light responses in plants and animals[1,2]. But the initial photochemical reaction of cryptochrome is still unclear. For example, although most photoreceptors are known to undergo light-dependent protein modification such as phosphorylation[3,4], no blue-light dependent phosphorylation has been reported for a cryptochrome. *Arabidopsis* cryptochrome 2 (cry2) mediates light regulation of seedling development and photoperiodic flowering[5,6]. The physiological activity and cellular level of cry2 protein are light-dependent[5–8], and protein–protein interactions are important for cry2 function[9,10]. Here we report that cry2 undergoes a blue-light-dependent phosphorylation, and that cry2 phosphorylation is associated with its

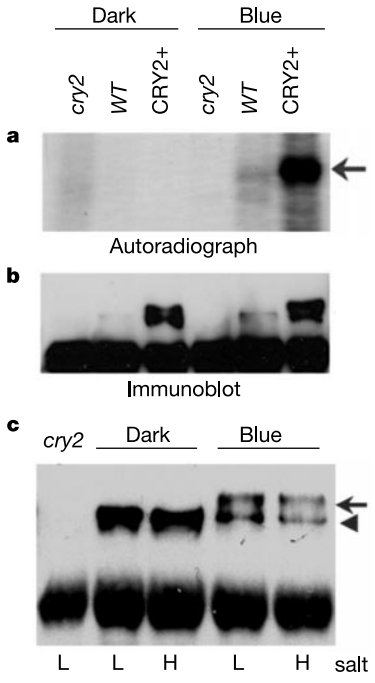

Figure 1 Blue-light-dependent phosphorylation of *Arabidopsis* cry2. **a**, Six-day-old seedlings were incubated with radioactive ^{32}P, exposed to blue light (5 μmol m^{-2} s^{-1}) for 10 min (Blue), or kept in the dark (Dark). Immunoprecipitation obtained using anti-CRY2 antibodies were separated in a 10% Laemmli gel, blotted, and exposed to an X-ray film. **b**, An immunoblot of **a** was probed with anti-CRY2 antibodies. **c**, Samples of 5-day-old wild-type seedlings with (Blue) or without (Dark) a 15-min blue-light treatment (5 μmol m^{-2} s^{-1}) were immunoprecipitated with anti-CRY2 antibodies in low-salt (100 mM NaCl, L) or high-salt buffer (200 mM NaCl, H) fractionated in a 10% NuPAGE gel, blotted, and probed with anti-CRY2 antibodies. In Figs 1–4, arrows indicate phosphorylated cry2; arrowheads indicate unphosphorylated cry2.

function and regulation. Our results suggest that, in the absence of light, cry2 remains unphosphorylated, inactive and stable; absorption of blue light induces the phosphorylation of cry2, triggering photomorphogenic responses and eventually degradation of the photoreceptor.

To test a hypothesis that the absorption of photons results in a biochemical modification of a cryptochrome molecule, we investigated whether *Arabidopsis* cry2 underwent a blue-light-induced phosphorylation *in vivo*. We fed etiolated (dark-grown) seedlings with radioactive phosphate ($^{32}PO_4^-$) before they were exposed to blue light, and then examined the cry2 phosphorylation. Autoradiography and immunoblot analysis of proteins purified by immunoprecipitation using anti-CRY2 antibody demonstrated that cry2 is phosphorylated in response to blue light (Fig. 1a, b). No radioactive cry2 was found in seedlings incubated in ^{32}P for 2 h in the dark, but ^{32}P-labelled cry2 was detected within 15 min of blue-light treatment. The level of radioactively labelled cry2 correlated with the amount of cry2 protein found in different genotypes (Fig. 1a, b). No cry2 or radioactively labelled immunoprecipitation product was detected in the *cry2* mutant, but both were found at higher levels in transgenic plants overexpressing cry2 than in the wild type. Although a similar level of cry2 is detected by immunoblot in CRY2+ transgenic plants irrespective of a brief light treatment, the ^{32}P-labelled cry2 was detected only in blue-light-treated seedlings (Fig. 1a, b).

Protein phosphorylation often causes slow migration of the phosphorylated protein in a SDS–polyacrylamide gel electrophoresis (PAGE) gel, allowing a more convenient analysis than the *in vivo* labelling experiments. A migration shift was only occasionally observed for the cry2 protein analysed using conventional Laemmli SDS–PAGE gels[11] (data not shown). Using a commercially available NuPAGE gel system (see Methods), two CRY2 isoforms were more consistently found in seedlings exposed to blue light, a fast-migrating band and a slow-migrating band, whereas only the fast-migrating CRY2 band was found in etiolated seedlings (Fig. 1c). The presence of the slow-migrating band found in blue-light-treated seedlings was not affected by a change in the ionic strength of the buffer used in the immunoprecipitation reaction (Fig. 1c), but it was eliminated by treating the sample with lambda phosphatase, which nonspecifically dephosphorylates proteins (see below).

We concluded that the slow-migrating band found in seedlings exposed to blue light is phosphorylated cry2, whereas the fast-migrating band from dark-grown or light-treated seedlings is unphosphorylated cry2. A significant fraction of cry2 remained unphosphorylated in plants exposed to blue light (Figs 1c and Fig. 2), suggesting that light-grown plants contain both phosphorylated and unphosphorylated cry2. Provided that one isoform is physiologically more active than the other one, the presence of both isoforms of cry2 in the cell may allow the total activity of cry2 to be adjusted rapidly in response to changing light conditions.

The light-induced phosphorylation of cry2 was detected shortly after seedlings were exposed to blue light (Fig. 2a, b). At a given fluence rate of light, the relative level of phosphorylated cry2 increased initially with the exposure time, but it decreased after a

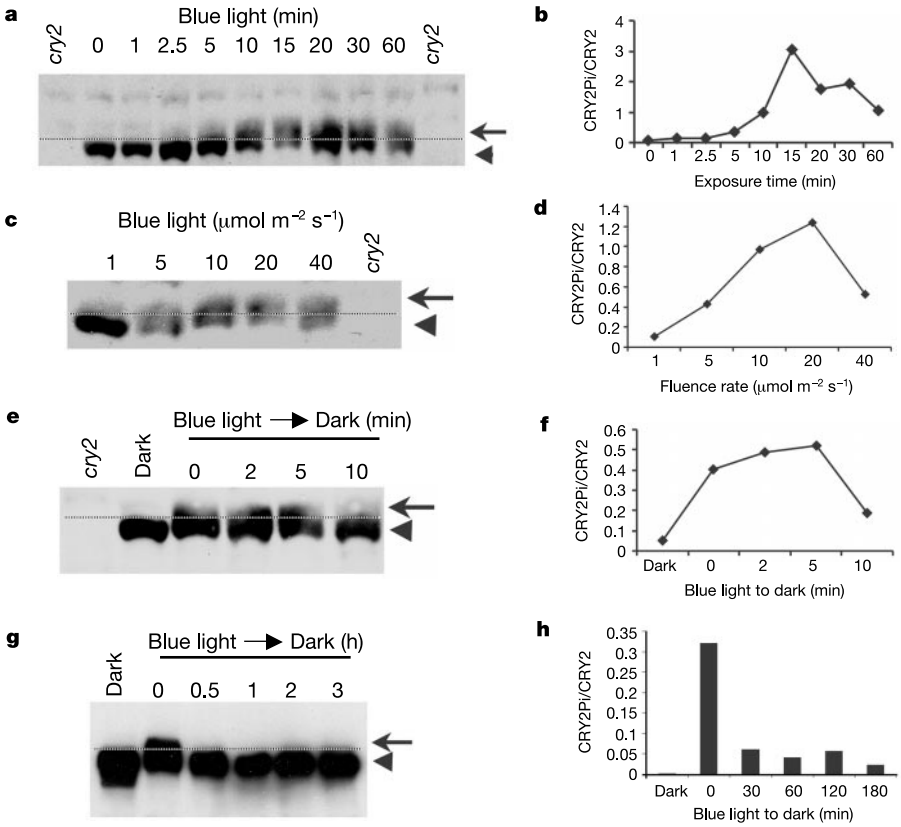

Figure 2 Kinetics analyses of light-dependent cry2 phosphorylation. Immunoblots in **a**, **c**, **e** and **g** were prepared in 10% NUPAGE gels and probed with anti-CRY2 antibodies. Samples of wild-type (**a**, **c**, **e**) or transgenic plants overexpressing *CRY2* (**g**) were analysed. Six-day-old dark-grown seedlings were treated in the following ways: **a**, **b**, exposed to blue light (5 μmol m^{-2} s^{-1}) for the periods indicated; **c**, **d**, exposed to blue light for 15 min at the fluence rates indicated; **e**, **f** exposed to blue light (5 μmol m^{-2} s^{-1}) for 10 min, and then transferred to the dark for the time indicated; **g**, **h**, exposed to blue light (5 μmol m^{-2} s^{-1}) for 20 min, and then transferred to the dark for the time indicated. The relative band intensities of phosphorylated cry2 (above the line) versus that of unphosphorylated cry2 (below) were presented as CRY2Pi/CRY2, and plotted in **b**, **d**, **f** and **h**, for the corresponding immunoblots shown in **a**, **c**, **e** and **g**, respectively.

prolonged blue-light treatment. The cry2 phosphorylation is fluence-rate-dependent (Fig. 2c, d). For a given time period of blue light treatment, relatively more cry2 phosphorylation was detected at higher fluence rates of blue light. However, a further increase of fluence rate resulted in a decrease in the relative amount of phosphorylated cry2. The level of phosphorylated cry2 decreased immediately after wild-type seedlings were transferred from blue light to dark, with little phosphorylated cry2 left shortly after plants were transferred to dark (Fig. 2e, f). Similarly, when CRY2 + transgenic seedlings were examined, the phosphorylated cry2 disappeared after blue-light-treated plants were transferred to dark (Fig. 2g, h).

The kinetic features of cry2 phosphorylation suggest that the phosphorylated cry2 is degraded, because the level of both total cry2 and phosphorylated cry2 declined in response to either increased exposure time or increased light intensity (Fig. 2)[5,7,12]. To further investigate this hypothesis, we screened for an *Arabidopsis* mutant that is impaired in cry2 degradation. Because a defect in the degradation of a photoreceptor might result in increased light responses, we examined blue-light-dependent cry2 degradation in *Arabidopsis* mutants that are known to exhibit either constitutive or hypersensitive light responses, including *cop1*, *cop9*, *det1*, *det2*, *det3*, *fus6* (*cop11*), *fus9* (*cop10*), *eid1*, and *sub1*[13–16]. An apparent defect of cry2 degradation was found only in the *cop1* mutant (Fig. 3). The *cop1* mutants are constitutively photomorphogenic[17]. Most *cop1* mutants are lethal except the two weak alleles, *cop1-4* and *cop1-6*[17,18]. Figure 3a showed that the cry2 degradation is partially impaired in both *cop1* mutants tested; higher levels of cry2 protein were detected in *cop1-4* and *cop1-6* seedlings than in the wild type under different blue-light conditions (Fig. 3a). In contrast, no obvious abnormality in light-induced cry2 degradation was found in the *det1-1* mutant (Fig. 3a), which, like the *cop1* mutant, also exhibits a light-independent de-etiolation response[17,19].

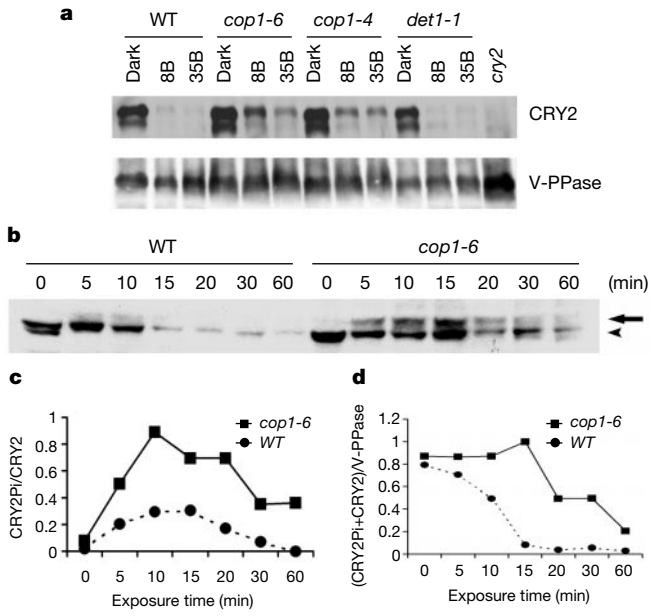

Figure 3 Accumulation of phosphorylated cry2 and impairment of cry2 turnover in cop1 mutants in response to blue light. **a**, Seven-day-old seedlings were exposed to blue light (8 μmol m^{-2} s^{-1} (8B) or 35 μmol m^{-2} s^{-1} (35B)] for two hours, and protein extracts were fractionated in a 10% Laemmli gel. The immunoblot was probed with anti-CRY2 antibody (CRY2), stripped and re-probed with antibodies against vacuole pyrophosphatase (V-PPase) for the loading control. **b**, Samples of 7-day-old wild-type (WT) or *cop1-6* seedlings, exposed to blue light (5 μmol m^{-2} s^{-1}) for the time periods indicated, were fractionated in a 10% NuPAGE gel and the immunoblot probed with anti-CRY2. **c**, Plots showing relative levels of phosphorylated cry2 versus unphosphorylated cry2 (CRY2Pi/CRY2) of samples from **b**. **d**, Plots showing total cry2 in samples from **b**, normalized using V-PPase signals (not shown) in the respective lane ((CRY2Pi+CRY2)/V-PPase).

The *COP1* gene encodes a putative subunit of an E3 ubiquitin ligase complex associated with proteolysis of the light-signalling transcription factor HY5 (ref. 20), and COP1 has been shown to physically interact with cryptochromes[10,21]. The exact role of COP1 in cry2 degradation is not clear, because blue-light-dependent cry2 degradation was still observed in *cop1* null alleles (data not shown). Nevertheless, regardless of the exact role of COP1 in cry2 degradation, the impairment of cry2 degradation in the *cop1* weak alleles allowed us to explore further the relationship between cry2 phosphorylation and cry2 degradation. We compared cry2 phosphorylation and cry2 degradation in wild-type plants and *cop1-6* mutant plants exposed to blue light for various time periods (Fig. 3b–d). It was found that a similar amount of unphosphorylated cry2 was detected in dark-grown *cop1-6* or wild-type seedlings. However, in seedlings exposed to blue light, the relative level of phosphorylated cry2 was significantly higher in the *cop1-6* mutant than in the wild type (Fig. 3b). A quantitative comparison of the relative amount of phosphorylated cry2 and the total amount of cry2 in the *cop1-6* mutant showed a correlation of a decrease of cry2 degradation and an increase of the relative abundance of phosphorylated cry2 (Fig. 3c, d).

Phytochromes have been shown to have protein kinase activity and to interact physically with cryptochromes[9,22,23]. Moreover, the function of *Arabidopsis* cry2 in the regulation of photoperiodic flowering is dependent on phyB[24], and cry2 has been shown to directly interact with phyB *in vivo*[9]. To investigate a possible involvement of phytochromes in cry2 phosphorylation, we first tested whether red light might induce cry2 phosphorylation. No cry2 phosphorylation was detected in seedlings exposed to red light (Fig. 4a) or far-red light (data not shown), which demonstrates the wavelength specificity of cry2 phosphorylation. We then investigated whether phytochromes might catalyse blue-light-dependent cry2 phosphorylation by testing cry2 phosphorylation in various phytochrome mutant lines. None of the monogenic phytochrome mutants tested, including *phyA*, *phyB*, *phyD*, *phyE* or the *cry1* mutant, had apparent defects in cry2 phosphorylation (Fig. 4c, and data not shown). To test a possibility that different phytochromes may act as cry2 kinases in a functionally redundant manner, we examined cry2 phosphorylation in the *phyAB* double mutant, and the *phyABD* and *phyBDE* triple mutants[25,26] (G.C.W., unpublished work), and the *hy1* mutant, which is impaired in phytochrome chromophore biosynthesis[27]. Again, cry2 phosphorylation was detected in all of these phytochrome mutants (Fig. 4b, c). A protein phosphatase treatment confirmed that the slow-migrating band of cry2 was indeed the phosphorylated form of cry2 (Fig. 4c).

It is somewhat surprising that the *phyBDE* triple mutant showed no obvious defects in cry2 phosphorylation, because phyB, phyD and phyE share a partial functional redundancy[25,26] and phyB can directly interact with cry2 (ref. 9). It seems unlikely that any single phytochrome species tested here is solely responsible for cry2 phosphorylation. However, our results do not exclude a possible phytochrome involvement in cryptochrome phosphorylation, because not all phytochrome mutants, and in particular, a null mutant lacking all five phytochromes, are currently available. Alternatively, cry2 phosphorylation may be catalysed by a non-phytochrome protein kinase.

The blue-light dependency of cry2 phosphorylation and a bell-shaped curve of the fluence-rate response of cry2 phosphorylation (Fig. 2d) indicate that the phosphorylated form of cry2 may represent physiologically active cry2. This is because the activity of cry2 in mediating blue-light-specific de-etiolation responses is limited primarily to low light-intensity conditions[5], in which relatively more phosphorylated cry2 was observed (Fig. 2a–d). It

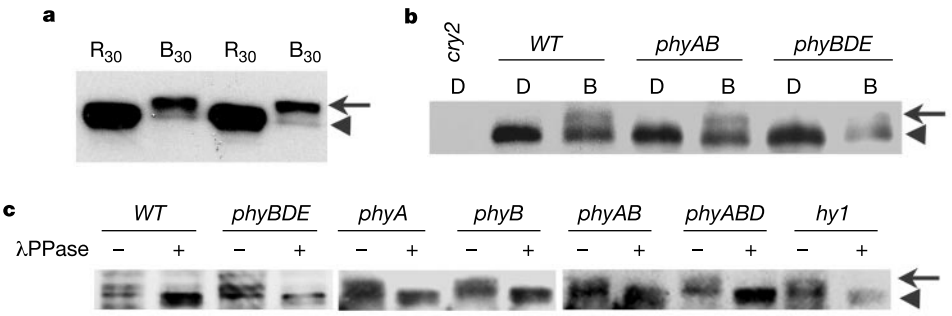

Figure 4 The lack of effect of red light or phytochrome mutations on cry2 phosphorylation. **a**, CRY2 overexpressing transgenic plants were exposed to red light (50 μmol m^{-2} s^{-1}), or blue light (5 μmol m^{-2} s^{-1}), for 30 min (R_{30}, B_{30}) or 60 min (R_{60}, B_{60}). **b**, Seedlings of the indicated genotypes were exposed to blue light (5 μmol m^{-2} s^{-1}) for 10 min (B) or left in dark (D). **c**, Seedlings of the indicated genotypes were exposed to blue light (5 μmol m^{-2} s^{-1}) for 10 min; samples were treated with (+) or without (−) lambda phosphatase (λPPase). Samples were fractionated in 10% NuPAGE gels and immunoblots probed with anti-CRY2 antibodies.

was found previously that expression of a GUS–CCT2 (CRY2 C-terminal domain) fusion protein caused a constitutive photomorphogenic phenotype in transgenic plants. For example, transgenic seedlings expressing GUS–CCT2 developed short hypocotyls in the dark or in the light, whereas wild-type plants exhibit inhibition of hypocotyl elongation only in response to light[28]. This observation indicates that a light-induced biochemical change may occur in the carboxy-terminal domain of cry2, resulting in activation of the photoreceptor[28].

We hypothesized that cry2 phosphorylation may occur in its C-terminal domain, in which several putative protein phosphorylation motifs are found (not shown). We further reasoned that the GUS–CCT2 fusion protein, which contains no chromophore-binding domain but is constitutively active, might show a constitutive phosphorylation regardless of light treatment. We tested this hypothesis by analysing phosphorylation of GUS–CCT2 fusion protein in etiolated or blue-light-treated transgenic plants expressing GUS–CCT2, using the *in vivo* ^{32}P-labelling immunoprecipitation assay (Fig. 5). In contrast to the endogenous cry2 that was phosphorylated only in blue-light-treated seedlings (Fig. 1a), the GUS–CCT2 fusion protein, immunoprecipitated by anti-GUS antibody, was labelled with ^{32}P in both dark-grown and blue-light-treated plants (Fig. 5). Residues of the GUS–CCT2 fusion protein that were phosphorylated must be in the CCT2 moiety because no phosphorylation was detected in GUS protein immunoprecipitated from transgenic plants expressing GUS (Fig. 5). This result indicates that the constitutive light response found in transgenic plants expressing the GUS–CCT2 fusion protein was due to a constitutive phosphorylation in the cry2 C-terminal domain of the fusion protein and that cry2 activity is dependent on the phosphorylation of its C-terminal domain.

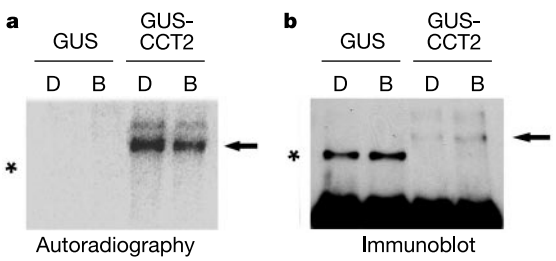

Figure 5 Constitutive phosphorylation of the CRY2 C-terminal domain moiety (CCT2) of the GUS–CCT2 fusion protein. The autoradiographs (**a**) and immunoblots (**b**) were prepared from the same nitrocellulose membrane, using the method as described in Fig. 1 except that the immunoprecipitation and immunoblot were reacted with anti-GUS antibodies. Transgenic plants expressing GUS (GUS) or GUS-CCT2 (GUS-CCT2)[28] were treated with (B) or without (D) blue light (5 μmol m^{-2} s^{-1}) for 20 min before harvesting. Arrows and asterisks indicate GUS–CCT2 and GUS, respectively.

Our results demonstrated that the function and turnover of *Arabidopsis* cryptochrome 2 is regulated by the blue-light-dependent phosphorylation. Because different cryptochromes have similar structures[1], it is likely that the blue-light-dependent phosphorylation is also important for the function of cryptochromes in other organisms. We propose that absorption of photons by a cryptochrome changes its conformation, enabling phosphorylation of the photoreceptor; the phosphorylated cryptochrome triggers signal transduction and physiological responses. The phosphorylation of a cryptochrome also marks it for degradation. The light-induced degradation of the active form of a cryptochrome may serve to regulate the cryptochrome activity in the presence of light and to de-sensitize the photoreceptor in the absence of light. □

Methods

Plant materials

Arabidopsis mutants and transgenic lines including *cry2-1* (ref. 6), GUS–CCT2 (ref. 28), *det1-1* (ref. 19), *cop1-4* and *cop1-6* (ref. 14), and the phytochrome mutants (*phyA-201*, *phyB-1*, *phyD-1*, *phyE-1*, *phyAB*) are as described[25] except for phyABD and phyBDE (G.C.W., unpublished work), The CRY2-overexpressing transgenic line in Col-4 background (CRY2+) was prepared as described[5]. Seeds treated with or without bleach-sterilization were sowed on MS medium (Sigma, M-9274) or in soil, respectively, kept in the dark at 4 °C for 3 days, exposed to white light for 4 h to promote germination, and grown in the dark for 5–7 days before use. Light sources are as described[24].

Immunoprecipitation and immunoblot analyses

For immunoprecipitation, seedlings were excised from the hypocotyl base under a dim red safe light (<5 μmol m^{-2} s^{-1}), and homogenized in ice-cold immunoprecipitation buffer (20 mM Tris-HCl pH 8, 150 mM NaCl, 1 mM EDTA, 10% glycerol, 0.2% Triton X-100, 10 μM NaF, 1 mM PMSF), and 1 × complete protease inhibitor cocktail (Roche). Extracts were passed through 0.2-μm filters. Antibodies were added (1:200) to the filtrate, incubated in ice for 1 h, protein-A-sepharose (Sigma) was then added (1:60) to the mixture and incubated in ice for 1 h. Immunoprecipitation complex was washed three times with ice-cold washing buffer (50 mM Tris-HCl pH 8, 140 mM NaCl, 1 mM EDTA, 0.1% Triton X-100), mixed with SDS–PAGE sample buffer, and boiled for 5 min.

Proteins were separated either in conventional 10% Laemmli gels using Tris-glycine buffer or in precast 10% Bis-Tris NuPAGE gels (NuPAGE NP0303, Invitrogen) using MOPS buffer according to the instructions of the manufacturer. NuPAGE gels were run at a constant voltage (100 V) at 13 °C for 6–7 h. Proteins were blotted to nitrocellulose membranes for autoradiographs or immunoblots. Immunoblots were probed with primary antibodies, and then with goat-anti-rabbit IgG conjugated with horseradish peroxidase (Amersham), and developed using the enhanced chemiluminescence (ECL) method as described previously[29]. Protein signals in an immunoblot were scanned, digitized and quantified using NIH Image. Different immunoblots are not directly comparable, because the exposure time of ECL cannot be precisely controlled between different experiments.

Phosphorylation assay

For *in vivo* labelling analyses, six-day-old, dark-grown seedlings (about 30) were cut from the hypocotyl base, incubated with ^{32}P (H_3PO_4 300 μCi, ICN) in water for 2 h in the dark at room temperature. The excess ^{32}P was removed by rinsing in water. Plantlets were treated under different light conditions before being collected for immunoprecipitation

and immunoblot analyses. For lambda phosphatase treatment, seedlings were homogenized in lambda phosphatase buffer provided by the manufacturer (New England Biolabs), and divided into two parts. One part was incubated without lambda phosphatase, the other part was incubated with 400 units of lambda phosphatase (New England Biolabs) at 30 °C for 30 min. The reactions were stopped by the addition of SDS–PAGE sample buffer, boiled and analysed by immunoblots as described.

Received 11 January; accepted 27 March 2002; doi:10.1038/nature00815.

1. Cashmore, A. R., Jarillo, J. A., Wu, Y. J. & Liu, D. Cryptochromes: blue light receptors for plants and animals. *Science* **284,** 760–765 (1999).
2. Sancar, A. Cryptochrome: the second photoactive pigment in the eye and its role in circadian photoreception. *Annu. Rev. Biochem.* **69,** 31–67 (2000).
3. Holmes, M. G. (ed.) *Photoreceptor Evolution and Function* (Academic, New York, 1991).
4. Briggs, W. R. & Huala, E. Blue-light photoreceptors in higher plants. *Annu. Rev. Cell Dev. Biol.* **15,** 33–62 (1999).
5. Lin, C. *et al.* Enhancement of blue-light sensitivity of *Arabidopsis* seedlings by a blue light receptor cryptochrome 2. *Proc. Natl Acad. Sci. USA* **95,** 2686–2690 (1998).
6. Guo, H., Yang, H., Mockler, T. C. & Lin, C. Regulation of flowering time by *Arabidopsis* photoreceptors. *Science* **279,** 1360–1363 (1998).
7. Ahmad, M., Jarillo, J. A. & Cashmore, A. R. Chimeric proteins between cry1 and cry2 *Arabidopsis* blue light photoreceptors indicate overlapping functions and varying protein stability. *Plant Cell* **10,** 197–208 (1998).
8. El-Din El-Assal, S., Alonso-Blanco, C., Peeters, A. J., Raz, V. & Koornneef, M. A QTL for flowering time in *Arabidopsis* reveals a novel allele of *CRY2*. *Nature Genet.* **29,** 435–440 (2001).
9. Mas, P., Devlin, P. F., Panda, S. & Kay, S. A. Functional interaction of phytochrome B and cryptochrome 2. *Nature* **408,** 207–211 (2000).
10. Wang, H., Ma, L. G., Li, J. M., Zhao, H. Y. & Deng, X. W. Direct interaction of *Arabidopsis* cryptochromes with COP1 in light control development. *Science* **294,** 154–158 (2001).
11. Laemmli, U. K. Cleavage of structural proteins during the assembly of the head of bacteriaphage T4. *Nature* **227,** 680–685 (1970).
12. Guo, H., Duong, H., Ma, N. & Lin, C. The *Arabidopsis* blue light receptor cryptochrome 2 is a nuclear protein regulated by a blue light-dependent post-transcriptional mechanism. *Plant J.* **19,** 279–287 (1999).
13. Fankhauser, C. & Chory, J. Light control of plant development. *Annu. Rev. Cell. Dev. Biol.* **13,** 203–229 (1997).
14. Kwok, S. F., Piekos, B., Misera, S. & Deng, X. W. A complement of ten essential and pleiotropic arabidopsis COP/DET/FUS genes is necessary for repression of photomorphogenesis in darkness. *Plant Physiol.* **110,** 731–742 (1996).
15. Buche, C., Poppe, C., Schafer, E. & Kretsch, T. *eid1*: A. new *Arabidopsis* mutant hypersensitive in phytochrome A-dependent high-irradiance responses. *Plant Cell* **12,** 547–558 (2000).
16. Guo, H., Mockler, T. C., Duong, H. & Lin, C. SUB1, an *Arabidopsis* Ca^{2+}-binding protein involved in cryptochrome and phytochrome coaction. *Science* **291,** 487–490 (2001).
17. Deng, X.-W., Caspar, T. & Quail, P. H. *COP1*: a regulatory locus involved in light-controlled development and gene expression in *Arabidopsis*. *Genes Dev.* **5,** 1172–1182 (1989).
18. McNellis, T. W. *et al.* Genetic and molecular analysis of an allelic series of cop1 mutants suggests functional roles for the multiple protein domains. *Plant Cell* **6,** 487–500 (1994).
19. Chory, J., Peto, C., Feinbaum, R., Pratt, L. & Ausubel, F. *Arabidopsis thaliana* mutant that develops as a light-grown plant in the absence of light. *Cell* **58,** 991–999 (1989).
20. Osterlund, M. T., Hardtke, C. S., Wei, N. & Deng, X. W. Targeted destabilization of HY5 during light-regulated development of *Arabidopsis*. *Nature* **405,** 462–466 (2000).
21. Yang, H. Q., Tang, R. H. & Cashmore, A. R. The signalling mechanism of *Arabidopsis* CRY1 involves direct interaction with COP1. *Plant Cell* **13,** 2573–2587 (2001).
22. Yeh, K. C. & Lagarias, J. C. Eukaryotic phytochromes: light-regulated serine/threonine protein kinases with histidine kinase ancestry. *Proc. Natl Acad. Sci. USA* **95,** 13976–13981 (1998).
23. Ahmad, M., Jarillo, J. A., Smirnova, O. & Cashmore, A. R. The CRY1 blue light photoreceptor of *Arabidopsis* interacts with phytochrome A *in vitro*. *Mol. Cell* **1,** 939–948 (1998).
24. Mockler, T. C., Guo, H., Yang, H., Duong, H. & Lin, C. Antagonistic actions of *Arabidopsis* cryptochromes and phytochrome B in the regulation of floral induction. *Development* **126,** 2073–2082 (1999).
25. Devlin, P. F. *et al.* Phytochrome D acts in the shade-avoidance syndrome in *Arabidopsis* by controlling elongation growth and flowering time. *Plant Physiol.* **119,** 909–915 (1999).
26. Devlin, P. F., Patel, S. R. & Whitelam, G. C. Phytochrome E influences internode elongation and flowering time in *Arabidopsis*. *Plant Cell* **10,** 1479–1488 (1999).
27. Parks, B. M. & Quail, P. H. Phytochrome-deficient *hy1* and *hy2* long hypocotyl mutants of *Arabidopsis* are deficient in chromophore biosynthesis. *Plant Cell* **3,** 1177–1186 (1991).
28. Yang, H.-Q. *et al.* The C termini of *Arabidopsis* cryptochromes mediate a constitutive light response. *Cell* **103,** 815–827 (2000).
29. Lin, C., Ahmad, M. & Cashmore, A. R. *Arabidopsis* cryptochrome 1 is a soluble protein mediating blue light-dependent regulation of plant growth and development. *Plant J.* **10,** 893–902 (1996).

Acknowledgements

We thank T. Cashmore, X.-W. Deng, J. Chory and T. Kretsch for providing *Arabidopsis* mutant lines. This work is supported by research grants from the National Institutes of Health, the National Science Foundation and UCLA-FGP. T.C.M. is supported by a predoctoral UCLA-NSF/IGERT training award.

Competing interests statement

The authors declare that they have no competing financial interests.

Correspondence and requests for materials should be addressed to C.L. (e-mail: clin@mcdb.ucla.edu).

Structure of the SRP19–RNA complex and implications for signal recognition particle assembly

Tobias Hainzl, Shenghua Huang & A. Elisabeth Sauer-Eriksson

Umeå Centre for Molecular Pathogenesis, Umeå University, SE-901 87 Umeå, Sweden

The signal recognition particle (SRP) is a phylogenetically conserved ribonucleoprotein. It associates with ribosomes to mediate co-translational targeting of membrane and secretory proteins to biological membranes. In mammalian cells, the SRP consists of a 7S RNA and six protein components. The S domain of SRP comprises the 7S.S part of RNA bound to SRP19, SRP54 and the SRP68/72 heterodimer; SRP54 has the main role in recognizing signal sequences of nascent polypeptide chains and docking SRP to its receptor[1–3]. During assembly of the SRP, binding of SRP19 precedes and promotes the association of SRP54 (refs 4, 5). Here we report the crystal structure at 2.3 Å resolution of the complex formed between 7S.S RNA and SRP19 in the archaeon *Methanococcus jannaschii*. SRP19 bridges the tips of helices 6 and 8 of 7S.S RNA by forming an extensive network of direct protein–RNA interactions. Helices 6 and 8 pack side by side; tertiary RNA interactions, which also involve the strictly conserved tetraloop bases, stabilize helix 8 in a conformation competent for SRP54 binding. The structure explains the role of SRP19 and provides a molecular framework for SRP54 binding and SRP assembly in Eukarya and Archaea.

The secondary structures of archaeal 7S RNAs are highly similar to their mammalian counterparts. These RNAs of about 300 nucleotides contain eight helical elements, which fold into the *Alu* and S domains connected by a long linker. Analyses of genome sequences indicate that archaeal species code for only two homologues of the six eukaryotic SRP proteins, namely SRP19 and SRP54 (ref. 6). In eubacteria, a minimal set of SRP subunits exists, and this is composed of 4.5S RNA, a single RNA helix with a region homologous to helix 8, and the SRP54 homologue Ffh.

SRP biogenesis in higher eukaryotes involves the sequential binding of SRP19 and SRP54 proteins to 7S RNA[4,5]. Archaeal SRP54 has an intrinsic affinity for 7S RNA *in vitro*, yet the presence of SRP19 significantly enhances SRP54 attachment[7]. The SRP19 binding site is situated in the apices of helices 6 and 8 of 7S RNA[8,9]. Binding of SRP19 leads to a restructuring of both helices, causing localized changes at the SRP54 binding site, which comprises the symmetric and asymmetric internal loops of helix 8 (refs 10, 11). Although crystal structures for helix 6 in complex with SRP19 (ref. 12) and helix 8 in complex with the M domain of Ffh[13] have been described, the protein–RNA and RNA–RNA interactions within the complete S domain of SRP were still unknown. We therefore determined the crystal structure of SRP19 bound to the S domain of RNA from *M. jannaschii*. Co-crystals of wild-type SRP19 in complex with a 97-nucleotide 7S.S RNA fragment, corresponding to helices 6 and 8, the U-turn, and part of helix 5, diffracted to 2.3 Å resolution and led to structure determination by molecular replacement (Fig. 1).

In the 7S.S RNA–SRP19 complex, RNA helices 6 and 8 associate in a parallel, slightly tilted mode. Helix 6 forms an overall rigid stem-loop structure with continuous base stacking (except for two looped-out adenosines, A176 and A177) and base pairing of canonical- or wobble-type throughout. In contrast, base mismatches in two regions of helix 8 cause a severe distortion from regular A-form RNA. Within the symmetric loop, bases C201–G205 and A216–A220 form five consecutive noncanonical base pairs.

14. Cao, Z., Henzel, W. J. & Gao, X. IRAK: A kinase associated with the interleukin-1 receptor. *Science* **271,** 1128–1131 (1996).
15. Zhang, F. X. *et al.* Bacterial lipopolysaccharide activates nuclear factor-κB through interleukin-1 signalling mediators in cultured human dermal endothelial cells and mononuclear phagocytes. *J. Biol. Chem.* **274,** 7611–7614 (1999).
16. Muzio, M., Ni, J., Feng, P. & Dixit, V. M. IRAK (Pelle) family member IRAK-2 and MyD88 as proximal mediators of IL-1 signalling. *Science* **278,** 1612–1615 (1997).
17. Fitzgerald, K. A. *et al.* Mal (MyD88-adapter-like) is required for Toll-like receptor-4 signal transduction. *Nature* **413,** 78–83 (2001).
18. Horng, T., Barton, G. M. & Medzhitov, R. TIRAP: an adapter molecule in the Toll signalling pathway. *Nature Immunol.* **2,** 835–841 (2001).
19. McCarthy, J. V., Ni, J. & Dixit, V. M. RIP2 is a novel NF-κB-activating and cell death-inducing kinase. *J. Biol. Chem.* **273,** 16968–16975 (1998).
20. Yan Liu, X. *et al.* Peptide-directed suppression of a pro-inflammatory cytokine response. *J. Biol. Chem.* **275,** 16774–16778 (2000).
21. Arron, J. R. & Choi, Y. Bone versus immune system. *Nature* **408,** 535–536 (2000).
22. Bundel, D. R. & Sigurskjold, B. W. Determination of accurate thermodynamics of binding by titration microcalorimetry. *Methods Enymol.* **247,** 288–305 (1987).
23. Otwinowski, Z. & Minor, W. Processing of X-ray diffraction data collected in oscillation mode. *Methods Enzymol.* **276,** 307–326 (1997).
24. Tong, L. REPLACE, a suite of computer programs for molecular-replacement calculations. *J. Appl. Crystallogr.* **26,** 748–751 (1993).
25. Brunger, A. T. *et al.* Crystallography & NMR system: A new software suite for macromolecular structure determination. *Acta Crystallogr. D* **54,** 905–921 (1998).
26. Jones, T. A., Zou, J.-Y., Cowan, S. W. & Kjeldgaard, M. Improved methods for building models in electron density maps and the location of errors in those models. *Acta Crystallgr. A* **47,** 110–119 (1991).
27. Evans, S. V. SETOR: hardware-lighted three-dimensional solid model representations of macromolecules. *J. Mol. Graph.* **11,** 134–138 (1993).
28. Nicholls, A., Sharp, K. A. & Honig, B. Protein folding and association: insights from the interfacial and thermodynamic properties of hydrocarbons. *Proteins* **11,** 281–296 (1991).
29. Haridas, V., Darnay, B. G., Natarajan, K., Heller, R. & Aggarwal, B. B. Overexpression of the p80 TNF receptor leads to TNF-dependent apoptosis, nuclear factor-κB activation, and c-Jun kinase activation. *J. Immunol.* **160,** 3152–3162 (1998).
30. Shevde, N. K., Bendixen, A. C., Dienger, K. M. & Pike, J. W. Estrogens suppress RANK ligand-induced osteoclast differentiation via a stromal cell independent mechanism involving c-Jun repression. *Proc. Natl Acad. Sci. USA* **97,** 7829–7834 (2000).

Supplementary Information accompanies the paper on *Nature*'s website (http://www.nature.com/nature).

Acknowledgements

We thank the structural biology groups at the Memorial Sloan-Kettering Cancer Center for use of the microcalorimeter; Z. Cao for human TRAF6 cDNA; G. Mosialos and E. Kieff for the human GST–CD40ct construct; L. Tong, R. Khayat, Z. Yang and C. Lima for help with diffraction data collection; G. Cheng for discussions; C. Ogata and MacCHESS staff for beamline access and support; T. Burling for maintaining the home X-ray source; V. Burkitt and A. Villa for technical help; and laboratory members of Imgenex for synthesizing the decoy peptides. This work was supported in part by the NIH (Y.C.), an MSTP grant (J.R.A.), start-up funds from the Department of Bioimmunotherapy (B.G.D.) and a Translational Research Grant from the Leukemia and Lymphoma Society (B.G.D.). H.Y. is a postdoctoral fellow from the Revson Foundation. H.W. is a Pew Scholar of biomedical sciences and a Rita Allen Scholar.

Competing interests statement

The authors declare that they have no competing financial interests.

Correspondence and requests for materials should be addressed to H.W. (e-mail: haowu@med.cornell.edu). The atomic coordinates have been deposited in the Protein Data Bank under accession numbers 1LB4 (native TRAF6), 1LB5 (TRAF6–TRANCE-R complex) and 1LB6 (TRAF6–CD40 complex).

erratum

Regulation of *Arabidopsis* cryptochrome 2 by blue-light-dependent phosphorylation

Dror Shalitin, Hongyun Yang, Todd C. Mockler, Maskit Maymon, Hongwei Guo, Garry C. Whitelam & Chentao Lin

Nature **417**, 763–767 (2002).

In Fig. 4a the third and fourth lanes should have been labelled R_{60} and B_{60} (not R_{30} and B_{30}). □